Use of Radiation Detection, Measuring, and Imaging Instruments to Assess Internal Contamination from Inhaled Radionuclides

Part III: Field Tests and Monte Carlo Simulations of Philips SKYLight Gamma Camera

Prepared by

R. Anigstein, R. H. Olsher, M. C. Erdman, and J. C. Engdahl

S. Cohen & Associates
1608 Spring Hill Road
Vienna, Virginia 2218

Under

Subcontract Number 30-06166-01

TKC Integration Services, LLC
6628 Brynhurst Drive
Tucker, Georgia 30084

Prepared for

Centers for Disease Control and Prevention
National Center for Environmental Health
Division of Environmental Hazards and Health Effects
Radiation Studies Branch

Under

Contract Number 200-2006-15696

Phillip Green
Project Officer

July 30, 2007

Contents

Tables

Figures

PREFACE

Part I of the present series describes a study to evaluate radiation detection and imaging systems commonly found in hospitals to determine their suitability for rapidly scanning individuals for internal contamination, and to develop recommendations regarding their potential use (Anigstein et al. 2007a). That report describes the measurement of count rates from single discrete radioactive sources of ^{60}Co, ^{137}Cs, ^{192}Ir, and ^{241}Am, using a Philips AXIS gamma camera, an Atomlab thyroid uptake system, and a Ludlum waste monitor. A Monte Carlo computer model of the Philips AXIS camera was developed and validated against the experimental in-air measurements. The model was then applied to calculating count rates on two models of the AXIS camera from radionuclides uniformly distributed in the lungs of a stylized mathematical phantom of the human body, based on the ORNL phantom series described by Cristy and Eckerman (1987).

Part II extends the earlier investigation by using realistic anthropomorphic phantoms to study the responses of four instruments to five radionuclides distributed in the lungs (Anigstein et al. 2007b). The experimental measurements were performed on a Rando Phantom—an anthropomorphic phantom that contains a human skeleton embedded in a tissue-equivalent urethane rubber. The five radionuclides—^{60}Co, ^{90}Sr, ^{137}Cs, ^{192}Ir, and ^{241}Am—were selected from the 10 nuclides cited by the DOE/NRC Interagency Working Group on Radiological Dispersion Devices as being among the "isotopes of greatest concern" (DOE/NRC 2003, Appendix F). Ten encapsulated sources of each nuclide were placed in pre-drilled holes in the lung region of the phantom. Count rates from each nuclide were measured on the Siemens e.cam Fixed 180 gamma camera, an Atomlab thyroid probe, a Ludlum survey meter, and a Ludlum waste monitor.

As described in Part II, the Los Alamos MCNPX (Monte Carlo N Particle eXtended) computer code was used to calculate calibration factors that relate count rates on these instruments to lung burdens of each of the five nuclides. A mathematical model of each of the instruments was constructed, using engineering drawings and other data obtained from the manufacturers. This model was combined with an MCNP model of a Rando Phantom, constructed from CT scans of this phantom (Wang et al. 2004). The combined model was used to simulate the response of each instrument to sources in the phantom, and the calculated results were compared with the experimental measurements. The agreement between the calculated and measured responses validated the MCNP models of the four instruments.

The current work extends the earlier investigations to the Philips SKYLight camera. The study was narrowed to three of the five radionuclides reported in Part II: ^{60}Co, ^{137}Cs, and ^{241}Am. As reported in Part II, the count rates from the ^{90}Sr sources recorded by the Siemens e.cam gamma camera were approximately 50% higher than the values calculated with the MCNP model. Preliminary studies on the Philips SKYLight camera also showed significant discrepancies, indicating a problem with the MCNP simulation of the production of bremsstrahlung x rays following the β decay of ^{90}Sr and its short-lived daughter, ^{90}Y. Therefore, further measurements and Monte Carlo simulations of ^{90}Sr were deferred to a forthcoming study that will attempt to resolve this problem. By the time of the present studies, the custom-made sources of ^{192}Ir, which

has a half-life of less than 74 days, had decayed to the point that very long counting times would have been required. Since the γ-ray energies of the three nuclides selected for this study bracket the energy range of ^{192}Ir γ rays, we judge that good agreement between the measurements and the MCNP simulations of these nuclides would be sufficient to validate the mathematical model of the Philips SKYLight camera. Our judgment is further supported by the observation that the MCNP model of the Siemens e.cam camera that produced reasonable agreement between the calculated and measured count rates from ^{60}Co, ^{137}Cs, and ^{241}Am also produced acceptable results for ^{192}Ir.

The present study encompassed measurements and corresponding MCNP simulations of sources of the three nuclides located in the lung region of a Rando Phantom, similar to the studies on the Siemens e.cam camera described in Part II. In addition, measurements and corresponding simulations were carried out on the source capsules in air, supported only by a shallow, light-weight, acrylic source holder that provided negligible shielding and attenuation of the photon radiation (but which was nevertheless included in the MCNP model).

The authors gratefully acknowledge the support and assistance of a number of individuals and organizations, without whom this work would not have been possible. These include Kenneth L. Miller, Professor of Radiology and Director of the Division of Health Physics at The Penn State Milton S. Hershey Medical Center, who arranged for access to the equipment in the Nuclear Medicine Division. X. George Xu, Associate Professor of Nuclear and Biomedical Engineering, Rensselaer Polytechnic Institute, provided the MCNP model of a Rando Phantom.

Several commercial firms provided valuable support and assistance. Philips Medical Systems, N. A., provided the design specifications and other data that enabled us to construct realistic models of the SKYLight cameras. Our special thanks go to Jody L. Garrard, Nuclear Medicine Product Manager; Mike Petrillo, Principal Engineer, SPECT Detector Engineering; and John Vesel, all of whom gave generously of their time and effort in support of this project. Lissa Tegelman of Isotope Products Laboratories designed the source capsules and facilitated the production and delivery of the custom-made sources on a very tight and aggressive schedule. Joshua Levy, president of The Phantom Laboratory, furnished advice and information, and donated spare parts for the Rando Phantom.

Chapter 1

RADIATION MEASUREMENTS

1.1 Introduction

Studies presented in Parts I and II of the present series of reports demonstrated that radiation detection and imaging systems commonly found in hospitals, including gamma cameras used in nuclear medicine, can be used to screen exposed individuals for radioactive materials inside the body. The current study extends the earlier investigation to the Philips SKYLight camera, a representative instrument of Philips Medical Systems, N. A., one of the three major U.S. suppliers of imaging equipment for nuclear medicine.[1]

The present chapter describes experiments to determine the response of this instrument to radioactive sources in air and in the lung region of the anthropomorphic Rando Phantom. The studies were performed at The Penn State Milton S. Hershey Medical Center in Hershey, PA.

1.2 Materials and Equipment

1.2.1 The Rando Phantom

The Rando Phantom used in the present study contains a natural human skeleton embedded in a urethane rubber. The rubber has an effective atomic number and mass density that closely simulate muscle tissue with randomly distributed fat. The Rando Phantom's lung material closely mimics the density of lungs in a median respiratory state. This phantom is similar to the one used by Anigstein et al. (2007b, Section 1.2.1), where it is described it in greater detail.

1.2.2 Radioactive Sources

The study addressed three radionuclides: ^{60}Co, ^{137}Cs, and ^{241}Am. These nuclides were among the five studied by Anigstein et al. (2007b).

The design of the Rando Phantom requires the use of discrete, encapsulated radioactive sources that can be inserted into the holes drilled in the phantom. Each custom-made source is sealed inside an acrylic rod, 1 cm long × 4.8 mm in diameter. Ten sources of each nuclide (the same sources used in the previous study) had been individually calibrated against NIST-traceable standards with a certified accuracy that range from ± 3.0% to ± 3.3% at the 99% confidence level.[2] The combined activities of the sources are presented in Table 1-1. A more detailed description of the sources is presented by Anigstein et al. (2007b, Section 1.2.2).

---

[1] The other two are Siemens Medical Solutions USA and GE Healthcare.

[2] Supplied by Isotope Products Laboratories, 24937 Avenue Tibbitts, Valencia, CA 91355.

Table 1-1. Radioactive Sources

Nuclide	Half-life (y)	Calibration date	Calibrated activity[a] (kBq)	Date of experiment	Decayed activity (kBq)
Co-60	5.271	6/7/05	43.80		34.5
Cs-137	30.07	9/14/05	78.2	3/31/07	75.5
Am-241	432.2	2/10/06	356		355

[a] Total activity of 10 sources of each nuclide

1.2.3 Philips SKYLight Gamma Camera

The Philips SKYLight gamma camera, illustrated in Figure 1-1, is a unique model that does not employ a gantry. The two camera heads can be positioned and oriented independently. The camera is equipped with a ⅜-inch-thick (0.95 cm) NaI(Tl) scintillator, in common with most of the gamma cameras in the United States. Up to 16 energy windows, with widths of up to 100%, can be used for acquisition of counts and/or images on this system. The counts displayed by the system are the sums of the counts in all the windows employed in a given acquisition. The system has a published energy range of 56 – 920 keV (Philips Medical Systems 2003). However, the acquisition software allows the user to set energy windows that include lower energies.

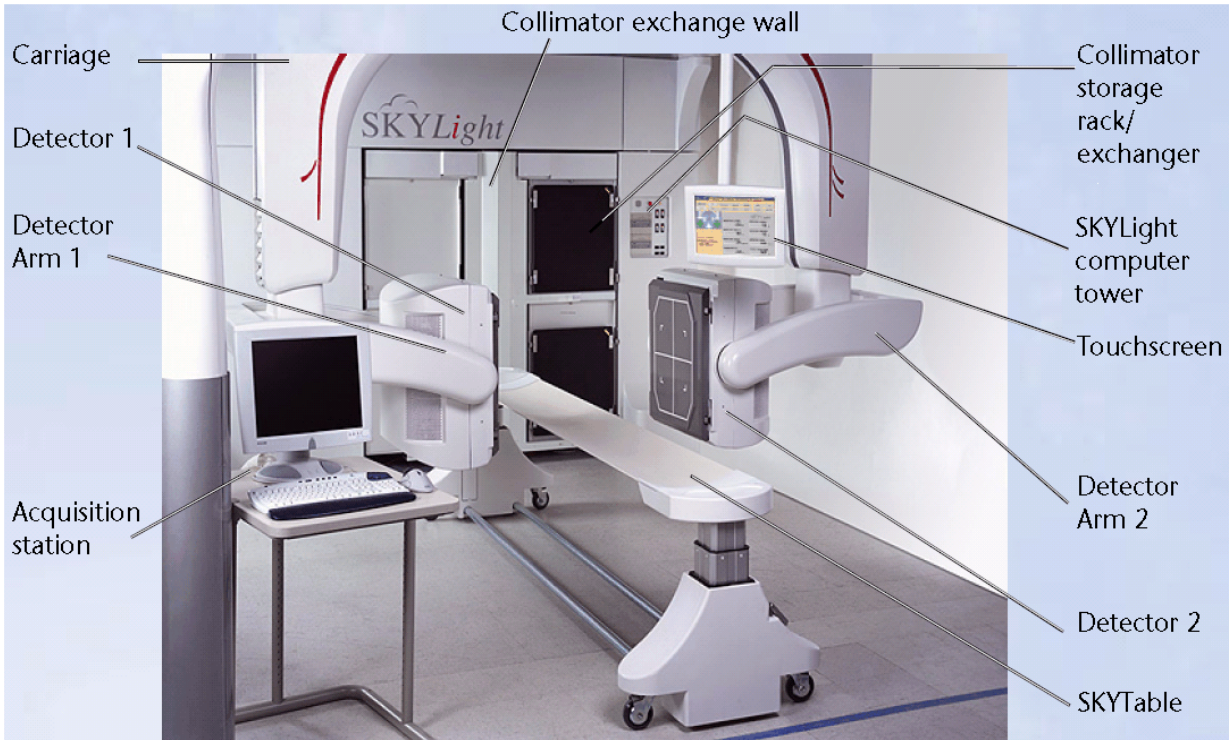

Figure 1-1. Philips SKYLight Imaging System (Philips Medical Systems 2004)

In order to maximize the count rate from a given nuclide, we took advantage of the wide range of possible energy windows in our initial experiments, using an energy range of 34 – 920 keV for measurements of ^{60}Co and ^{137}Cs. However, the observed counts were significantly lower than the corresponding MCNP simulations.

The discrepancy is explained if we note that routine nuclear medicine clinical applications do not require simultaneous imaging of isotopes with energies below 100 keV and above 500 keV. Therefore, most systems automatically select a high voltage (HV) to define a gain range that is linear for the selected energy windows. When high-energy windows are selected, the HV is lowered to encompass the higher energy signals. When only low-energy windows are employed, the HV is raised to increase the amplitude of the signals, which improves imaging performance. Since there are lower level thresholds that are hard-wired into these circuits, when the HV is set to a lower range low-energy events that might otherwise be measurable with the higher HV setting are now eliminated because they fall below the predefined lower thresholds. Although this is not explicitly described in the user's manual, we are reliably informed that the Skylight does function in this manner, as do the other competitive manufacturers' systems. We simulated this effect by raising the lower end of the energy range in the MCNP analysis from 34 keV to 123 keV, which essentially resolved the discrepancies between the measurements and the calculations.

We repeated the study using a narrower range of energy windows. Two sets of energy windows were used for both ^{60}Co and ^{137}Cs. One set comprised two contiguous 86% energy windows. For such settings, the upper limit of the upper window is ~6.3 times the lower limit of the lower window. Based on our analysis of the initial experiments, such an energy range should not cause a rejection of events at the low end of the range. To confirm that such a range did not produce anomalous results, we also performed measurements on these two nuclides using a single 100% energy window. For such settings, the upper limit is 3 times the lower limit.

The energy range for each nuclide was selected to produce the maximum counts for the given ratio of upper and lower energy limits, based on spectra generated by MCNP simulations of sources in the Rando Phantom. Because of the narrow range of the ^{241}Am spectrum, only one set, comprising a single 83% window, was used for this nuclide. Table 1-2 lists the windows in each set, the peak or central energy for each window, the upper and lower energy limits, and the width, expressed in percent of the peak energy.

Table 1-2. Energy Windows (keV)

Nuclide:		Co-60				Cs-137				Am-241			
Set No.	Window	Peak	Min	Max	Width	Peak	Min	Max	Width	Peak	Min	Max	Width
1	1	124.6	71.0	178.2	86%	191.2	109.0	273.4	86%	51.3	30.0	72.6	83%
	2	312.6	178.2	447.0	86%	479.6	273.4	685.8	86%				
2	1	198.0	99.0	297.0	100%	184.0	92.0	276.0	100%				

1.3 Radiation Measurements

Measurements were performed with the SKYLight camera, using both detectors with the collimators removed. In the first set of measurements, the 10 sources of each nuclide were placed in an acrylic holder, 9.8 cm × 1.27 cm × 0.63 cm thick. The sources were placed in holes that were 3.2 mm deep, spaced 9.5 cm apart. Since the activity was about 7 mm from the lower end of the source, the holder provided negligible shielding or attenuation of the photons in the energy ranges used in the experiments. The source holder was centered both horizontally and vertically between the two camera heads, which were separated by 27 cm, the distance needed to accommodate the Rando Phantom used in the next set of measurements. Background counts were taken before and after measurements with each set of energy windows. The reported counts are the average of the background-corrected counts in each detector.

In the second set of measurements, the Rando Phantom was centered between the two detectors. The height of the stand was adjusted so that the position of the phantom was similar to that of a patient undergoing a planar lung scan, with the two detectors recording anterior and posterior views. The front and back of the phantom were approximately 5 cm from the aluminum windows covering the detectors. Such a separation would be needed in the event that the camera were used to assess an exposed individual: without a collimator, there is no pressure-sensitive alarm to protect the patient from potential injury by contact with the detector, nor to protect the detector from being damaged by contact with the patient.

Background counts, with the phantom in position but without sources, were taken before and after measurements with each set of energy windows. Two sets of measurements were taken. First the phantom faced detector 1, with its back to detector 2. Next, the phantom was turned to face detector 2. The reported counts for each view are the average of the background-corrected counts in each detector.

Chapter 2

MONTE CARLO SIMULATIONS OF EXPERIMENTAL MEASUREMENTS

In this chapter, we discuss the use of Monte Carlo computer models to simulate the experimental measurements presented in Chapter 1. The first step of the analysis was to construct a mathematical model of the SKYLight camera. We then simulated the radiation response of this model, using the same exposure geometries described in Chapter 1, and compared the calculated results to the experimental observations. The aim of these comparisons is to validate the model of the camera. As will be discussed in a later report in the present series, this model will be used to derive calibration factors for this camera, enabling the camera to be used for assessing the intakes and doses to exposed individuals.

2.1 Methodology

The methodology was essentially the same as used in the Monte Carlo simulations of the Siemens e.cam gamma camera using the MCNPX computer code, as described by Anigstein et al. (2007b, Chapter 2). A summary description is presented here, with emphasis on differences with the previous analysis.

2.1.1 MCNP Model of Rando Phantom

Wang et al. (2004) created an MCNP voxel model of a Rando Phantom based on data from a CT scan of the phantom. The phantom, similar to the one used our experiments, represented the torso of an adult male.

White (1978) lists the elemental composition of lung and muscle in the Rando Phantom. The elemental composition of hydrated cortical bones of adults is listed in ICRP 1995, Table 27. We incorporated these compositions, listed in Table 2-1, into the model created by Wang et al. to replicate the Rando Phantom used in our studies.

2.1.2 Model of Philips SKYLight Gamma Camera

A model of the Philips SKYLight Gamma Camera was constructed on the basis of engineering drawings and other data obtained from the manufacturer. Some of the information is proprietary and confidential—such information can be discussed only in general terms.

Similar to other gamma cameras used for SPECT (single photon emission tomography) studies and for planar images, the SKYLight consists of a large planar NaI(Tl) crystal, optically coupled to a glass plate that in turn is coupled to an array of PMTs. The entire assembly is enclosed on five sides by a heavy lead shield to prevent stray radiation from reaching the crystal. The camera system imposes an electronic mask over the crystal that creates a dead zone in the margins. Thus, scintillation events near the edges of the crystal which cannot be properly localized by the PMTs are not counted. The active area of the crystal, called the intrinsic field of view, is

indicated by the octagonal outline on the face of detector 2 in Figure 1-1. The overall dimensions of the field of view are 50.8 cm high × 38.0 cm wide. The actual area is smaller than the product of these dimensions, due to the octagonal shape.

Table 2-1. Tissue Composition of Rando Phantom (%)

Element	Lung[a]	Muscle[a,b]	Skeleton[c]
H	5.74	8.87	3.4
C	73.94	66.81	15.5
N	2.01	3.10	4.2
O	18.14	21.13	43.5
Na			0.1
Mg			0.2
P			10.3
S			0.3
Ca			22.5
Sb	0.16	0.08	
Density (g/cm^3)	0.32	1.00	1.92

[a] White (1978)

[b] All regions of phantom other than lungs or skeleton

[c] ICRP 1995, Table 27

The MCNP model of the gamma camera exposure geometry replicated the conditions of the experiment, described in Section 1.3. Figure 2-2 is a sagittal section that shows the position of the voxel model of the Rando Phantom with respect to the two heads of the gamma camera.

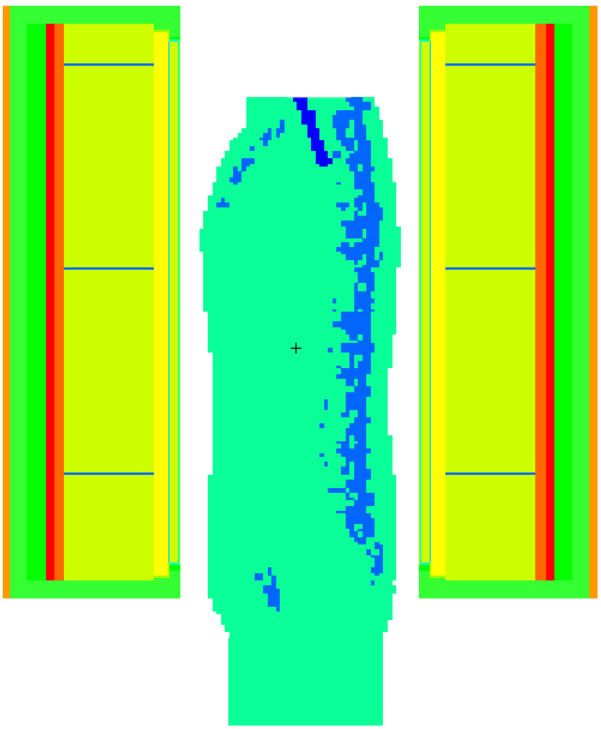

Figure 2-2. Sagittal Section of MCNP Model of Rando Phantom and Philips SKYLight

2.2 Comparison of MCNP Simulations with Experimental Measurements

The results of the MCNP analyses of the gamma camera are listed in Table 2-2, together with the observed count rates.

Table 2-2. Count Rates on Philips SKYLight Gamma Camera (cps/Bq)

Nuclide	Exposure Geometry	Set No.[a]	MCNP		Experiment		Difference (%)[b]	
			Anterior	Posterior	Anterior	Posterior	Anterior	Posterior
Co-60	Source holder	1	0.0730	—	0.0686	—	6.4%	—
		2	0.0520	—	0.0487	—	6.6%	—
	Rando Phantom	1	0.1166	0.1403	0.1171	0.1243	-0.4%	12.9%
		2	0.0833	0.1007	0.0846	0.0899	-1.5%	11.9%
Cs-137	Source holder	1	0.0757	—	0.0743	—	1.8%	—
		2	0.0364	—	0.0363	—	0.3%	—
	Rando Phantom	1	0.0732	0.0929	0.0801	0.0891	-8.6%	4.2%
		2	0.0521	0.0640	0.0573	0.0628	-9.1%	1.9%
Am-241	Source holder	1	0.0764	—	0.0751	—	1.8%	—
	Phantom	1	0.0357	0.0403	0.0348	0.0402	2.8%	0.2%

[a] Set of energy windows, specified in Table 1-2

[b] MCNP ÷ Experiment − 1

We observe that the use of narrower energy windows (set number 2) for ^{60}Co and ^{137}Cs does not lead to significantly better agreement between the calculated and the measured count rates. Since the wider energy ranges increase the count rates and therefore the sensitivity of the instrument, we will employ these ranges in determining the recommended calibration factors for this instrument, which will be presented in a later report in the present series.

Overall, Table 2-2 shows reasonable agreement between the calculated and experimental values. The root-mean-square (rms) difference between the calculated and measured values of the normalized count rates from the sources in the source holder is 4.3%, while the rms difference between the values of both anterior and posterior views of the Rando Phantom is 7.0%.[3] The statistical uncertainties make a negligible contribution to the discrepancy. Given other sources of experimental error, including the uncertainty in the activities of the sources, the exact compositions and densities of the constituents of the Rando Phantom used in the experiment, and some observed anatomical differences between the experimental and voxel phantoms, we conclude that the MCNP model has been validated for these three nuclides.

[3] The rms difference is calculated as $\Delta_{rms} = \sqrt{\frac{\sum_{i=1}^{n} \delta_i^2}{n}}$, where δ_i is the % difference between the calculated and experimental values, and n = 5 for the source holder, 10 for the Rando Phantom.

REFERENCES

Anigstein, R., et al. 2007a. "Use of Radiation Detection, Measuring, and Imaging Instruments to Assess Internal Contamination from Inhaled Radionuclides. Part I: Feasibility Studies." http://www.bt.cdc.gov/radiation/pdf/hospitalinstruments.pdf

Anigstein, R., R. H. Olsher, and J. C. Engdahl. 2007b. "Use of Radiation Detection, Measuring, and Imaging Instruments to Assess Internal Contamination from Inhaled Radionuclides. Part II: Field Tests and Monte Carlo Simulations Using Anthropomorphic Phantoms."

Cristy, M., and K. F. Eckerman. 1987. "Specific Absorbed Fractions of Energy at Various Ages from Internal Photon Sources. I. Methods," ORNL/TM-8381/V1. Oak Ridge, TN: Oak Ridge National Laboratory.

The DOE/NRC Interagency Working Group on Radiological Dispersal Devices (DOE/NRC). 2003. "Radiological Dispersal Devices: An Initial Study to Identify Radioactive Materials of Greatest Concern and Approaches to Their Tracking, Tagging, and Disposition." www.ssa.doe.gov/sp70/documents/RDDRPTF14MAY03.pdf.

International Commission on Radiological Protection (ICRP). 1995. "Basic Anatomical and Physiological Data for Use in Radiation Protection: The Skeleton," ICRP Publication 70. *Annals of the ICRP, 25*(2). Oxford: Pergamon Press.

Philips Medical Systems. 2003. "SKYLight™ Camera and Collimator Specifications." http://www.medical.philips.com/main/products/nuclearmedicine/assets/images/skylight/SKYLight_specs.pdf

Philips Medical Systems. 2004. "SKYLight® Imaging System User's Manual: A Manual Describing How to Use the SKYLight Imaging System."

Wang, B., X. G. Xu, and C. H. Kim. 2004. "A Monte Carlo CT Model of the Rando Phantom." *American Nuclear Society Transactions*, *90*, 473-474.

White, D. R. 1978. "Tissue Substitutes in Experimental Radiation Physics." *Medical Physics, 5*(6), 467–479.